

FIG. 8.— Illustrating fluxes and velocities of the individual components listed in Table 1 without the effect of the PSF. The arrows show the fluxes and velocities assigned to the spiral arms which are fixed at  $-37''$  and  $33''$  galactocentric distance. Filled boxes illustrate the nucleus, crosses the jet, and diamonds the cloud, respectively.

indicate a rather strong gradient within the nuclear disk (see Table 1), or, as mentioned, a difference in line ratios between an eventual absorbed counter-jet and Disk 2.

The disk rotates in the potential of the stellar bulge at an angle to the kinematic symmetry plane of the bulge. Our slit is oriented close to the kinematic major axis of the disk, but close to the kinematic minor axis of the stellar bulge (Dumas et al. 2007). The redshift of the central source in our model and the systematic redshift of the stellar bulge differ with about  $100 \text{ km s}^{-1}$  (Fig. 3). The slit crosses the spiral arms close to the photometric minor axis of the outer galactic disk (Fig. 1). Their mean velocity relative the nucleus is  $-87 \text{ km s}^{-1}$ . In view of the fact that our slit is parallel to the line of nodes of the emission line velocity field and perpendicular to the line of nodes of the stellar velocity field, the difference in central velocity between our models and that of the stellar bulge, as seen in Fig. 3, may be accounted for if our slit misses the central peak passing about  $1''$  to the South of the nucleus. This would mean that our derived rotation curve is somewhat flatter than the true one and the intensities of the central source too faint. The NaD absorption lines, measured with SPLOT, show the same systematic redshift as the emission lines, which would

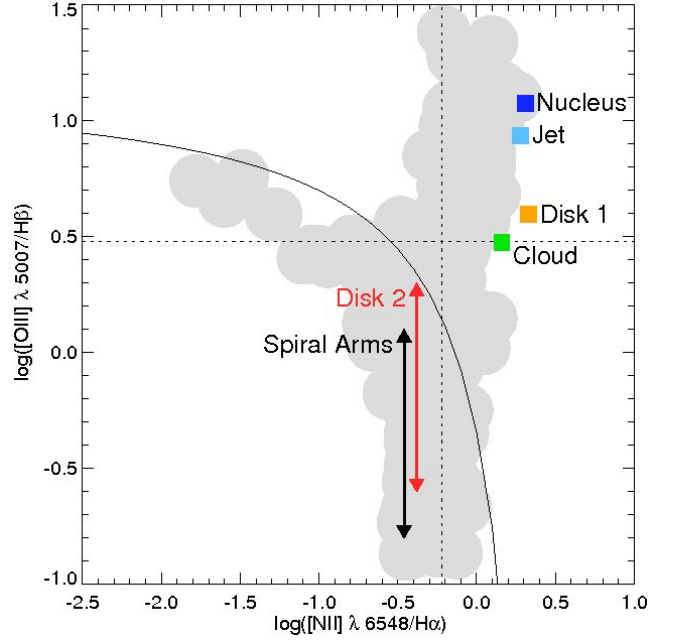


FIG. 9.— Line ratio diagnostics derived from our ESO spectra. The solid curve shows the Starburst-AGN separation lines of Kewley et al. (2001), with the shaded region indicating their sample galaxies.

imply that their main absorption comes from the emission line disk and not from the stellar bulge. The negative mean velocity of the spiral arms speaks somewhat against this miscentering view with whatever weight this may have.

## 7. CONCLUSIONS

We want to stress that our method, i.e. because of the necessity to introduce number of more or less reasonable assumptions in order to decrease the number of free parameters, does not give a unique solution to the nuclear structure of NGC 1358. The differing velocities in the different lines give strong constraints for the line ratios. Experiments with our model, for example, shows that it is the weakness of [OIII] in the postshock cloud and nuclear disk that causes the dip in velocity of the Eastern part of the velocity curve to be deeper in [OIII], and the [OIII] velocity curve to be flatter on both sides. But, it is necessary to know with good precision the outer wings of the PSF in order to account for the influence of the strong components on the fainter ones.

In our particular case the main draw back is that the observations are restricted to a single slit. To get all necessary information about the velocities and spatial distribution of the different components from an isolated spectrum is futile, because of the very limited coverage and the unknown influence due to the point spread function from sources outside the slit. By adding more slits, there is still a difficulty to obtain an accurate and complete coverage (Lindblad et al. 1996). Obviously, the ideal is an integral field spectrometer and an extension of the method to a two-dimensional treatment, combined with comprehensive statistical analysis, covering the entire region of interest.

Nevertheless, we argue that, with this analysis, we have made a step towards a resolution of the nuclear region of NGC 1358 into a number of different components with